Mathematical Biosciences and Engineering

http://www.aimspress.com/journal/MBE

MBE, 18(6): 8374–8391.
DOI: 10.3934/mbe.2021415
Received: 13 June 2021
Accepted: 12 September 2021
Published: 27 September 2021

Research article

Mathematical modeling of the influence of cultural practices on cholera infections in Cameroon

Eric Che[1,*], Eric Numfor[2], Suzanne Lenhart[3] and Abdul-Aziz Yakubu[1]

[1] Department of Mathematics, Howard University, Washington, DC 20059, USA
[2] Department of Mathematics, Augusta University, Augusta, GA 30912, USA
[3] Department of Mathematics, University of Tennessee, Knoxville, TN 37996, USA

* **Correspondence:** Email: ericngangche@yahoo.com.

Abstract: The Far North Region of Cameroon, a high risk cholera endemic region, has been experiencing serious and recurrent cholera outbreaks in recent years. Cholera outbreaks in this region are associated with cultural practices (traditional and religious beliefs). In this paper, we introduce a mathematical model of the influence of cultural practices on the dynamics of cholera in the Far North Region. Our model is an SEIR type model with a pathogen class and multiple susceptible classes based on traditional and religious beliefs. Using daily reported cholera cases from three health districts (Kaélé, Kar Hay and Moutourwa) in the Far North Region from June 25, 2019 to August 16, 2019, we estimate parameter values of our model and use Akaike information criterion (AIC) to demonstrate that our model gives a good fit for our data on cholera cases. We use sensitivity analysis to study the impact of each model parameter on the threshold parameter (control reproduction number), $\mathcal{R}_c$, and the number of model predicted cholera cases. Finally, we investigate the effect of cultural practices on the number of cholera cases in the region.

Keywords: cultural practices; ODE cholera model; cholera data; Far North region of Cameroon

1. Introduction

According to the World Health Organization (WHO), cholera is an acute intestinal infection caused by ingestion of food or water contaminated with the bacterium *Vibrio cholerae* [1]. In many parts of the world, cholera remains a significant threat to public health [2]. It continues to devastate impoverished populations with limited access to medication, clean water and proper sanitation amenities [3]. Annually, about 1.3–4.0 million cholera cases and 21,000–143,000 cholera-induced deaths are reported worldwide [1,4]. In recent years, there has been several reports of major cholera outbreaks. For example, in Yemen from 2016–2017 cholera outbreak led to more than one million cases. Major outbreaks

were also reported in Haiti (2010–2012), Sierra Leone (2012), Ghana (2011), Nigeria (2010), Vietnam (2009), Zimbabwe (2008), and India (2007). Cameroon, a cholera endemic African country experienced large cholera outbreaks in 1991, 1996, 1998, 2004, 2010 and 2011 [5]. In 2017, 1,227,391 cases and 5654 cholera-related deaths were reported from 34 countries [6].

In recent years, the Far North Region of Cameroon has been experiencing serious recurrent cholera outbreaks, and these outbreaks are linked to cultural practices (traditional and religious beliefs) of the people of this region. The impact of traditional and religious practices on the spread of infectious diseases is a known fact in the literature. For example, in 2015, A. Manguvo and B. Mafuvadze in their study demonstrated that the transmission of Ebola in West Africa is linked to traditional and religious practices [7]. In 2017, Ngwa et al. [8] carried out a field study that demonstrate that cultural practices in the Far North region influence cholera transmission. The high cholera attack rate in mountainous areas was attributed to cultural practices such as mountain burial. They also noted that many people in the Far North had limited scientific knowledge about the cholera disease and its transmission. Rich cultural practices are common in villages and urban areas of the Far North Region of Cameroon. For example, the tradition of communal eating from the same plate and drinking from the same cup is common place [9]. In addition to cultural practices, other factors that contribute to cholera cases include the lack of clean drinking water and poor health facilities.

Transmission of cholera can be indirect, from a water source containing the bacterium to susceptible humans, or direct, from infectious humans to susceptible humans. Several continuous-time mathematical ODE models have been developed in an effort to gain a deeper understanding of cholera transmission dynamics, see for example [10–14] and the citations therein. In a recent paper, Che et al. introduced a continuous-time ODE low-high risk structured cholera model and used it to capture the annual reported cholera infections in Cameroon from 1987 to 2017 [15]. Furthermore, using the fitted risk structured cholera model, they studied the impact of three intervention strategies (vaccination, treatment and improved sanitation) on the number of cholera infections in Cameroon from 2004 to 2022.

Education can also serve as a disease intervention strategy. For example, Al-arydah et al. in [16] formulated and analyzed a mathematical model that includes two essential and affordable control measures: water chlorination and education. Cholera education includes advising people with symptoms to seek medical care promptly, and improving sanitation and hygienic practices. In the Far North Region of Cameroon, even with education, some people still maintain their traditional and religious practices which are sometimes in conflict with proper cholera hygiene [8].

In this paper, we formulate a mathematical model of the influence of cultural practices on cholera infections in the Far North Region of Cameroon. We compute the control reproduction number, $\mathcal{R}_c$, and using cumulative reported cholera cases for June 25–August 16, 2019 from three health districts (Kaé lé, Kar Hay and Moutourwa) in the Far North Region (from the Cameroon Ministry of Public Health) [17], we estimate model parameter values and demonstrate that our model captures the dynamics of the cholera infections. Also, we use sensitivity analysis to study the impact of each model parameter on the threshold parameter, $\mathcal{R}_c$, and the number of model predicted cholera cases.

The rest of the paper is organized as follows: In Section 2, we formulate our mathematical model with different susceptible classes representing cultural practices and with vaccination, and compute the control reproduction number $\mathcal{R}_c$. Also, we study the reduced model without cultural practices and vaccination. Using the cumulative cholera cases from three health districts in the Far North Region, we

fit the parameters to the cumulative cases. Using the Akaike information criterion (AIC), we illustrate that in the Far North Region of Cameroon, our model with cultural practices and with vaccination (in comparison with the model without cultural practices and vaccination) gives a better fit for the cumulative cholera cases. In Section 3, we use sensitivity analysis to study the impact of each model parameter on the threshold parameter, $\mathcal{R}_c$, and the number of model predicted cholera cases. The discussion of our results and conclusions are presented in Section 4.

2. Model with culture

Here, we formulate a model that captures the influence of cultural practices on the dynamics of cholera in the Far North Region, a high risk cholera region [15] of Cameroon. Our model is based on the schematic diagram shown in Figure 1. The list of the model variables and their descriptions are in Table 1, while the parameters are in Table 3. In our model, $S(t)$ represents susceptible humans, $E(t)$ represents exposed humans, $I(t)$ represents infectious humans and $R(t)$ represents recovered individuals at time $t \geq 0$. Also, $B(t)$ represents the concentration of pathogen in the contaminated water at time t. To investigate the impact of cultural practices on the dynamics of cholera infections in the Far North Region, we partition the susceptible human subpopulation S into three classes: those who are not careful in practicing safe cholera intervention measures and not willing to be vaccinated as a result of their cultural beliefs (S_r), those who are careful in practicing safe cholera intervention measures but are not willing to be vaccinated (S_c) and those who are careful in practicing safe cholera intervention measures and are willing to be vaccinated (S_v), so that $S = S_r + S_c + S_v$. The size of the total human population at time t is

$$N(t) = S_r(t) + S_c(t) + S_v(t) + E(t) + I(t) + R(t).$$

At time $t \geq 0$, individuals in the S_r, S_c and S_v classes are recruited (by birth or immigration) at rates $\alpha\beta$, $\alpha_c\beta$, $\alpha_v\beta$ respectively, where β is the constant recruitment rate and α, α_c and α_v are proportional constants in $(0, 1)$, and $\alpha + \alpha_c + \alpha_v = 1$. Individuals in the S_r, S_c and S_v classes become infected either by contact with infectious individuals (direct transmission) at rates ρ_r, ρ_c and ρ_v, respectively, or through contact with contaminated water (indirect transmission) at rates β_r, β_c and β_v, respectively. We assume that individuals in the S_r class have higher direct transmission rates than those in the S_c and S_v classes, and that susceptible individuals in the S_v class are vaccinated at rate v. The vaccinated individuals progress to the recovered class. Following contact with infectious individuals or contaminated water, the susceptible individuals may become exposed to the infection. The time period from cholera pathogen exposure to the development of symptoms (incubation period) is relatively short, varying from about 12 hours to five days [1]. During the pathogen incubation period, exposed individuals are not infectious and do not shed pathogen into the water compartment. However, surviving exposed individuals may progress to the infectious class after the pathogen incubation period at rate σ. Infectious individuals can contaminate the water by shedding the cholera pathogen at rate ξ. An infectious individual can thus generate secondary infections in two ways: through direct contact with susceptible individuals, and by first shedding the pathogen into the water compartment, where it can eventually infect susceptible individuals. We assume that in Cameroon, the number of cholera infections from cholera infected corpses is very small and can thus be ignored. Cholera is a treatable disease. In Cameroon cholera is usually treated with oral rehydration salt solutions and antibiotics. In

our model, infectious individuals can progress to the recovered class at rate γ. However, recovered individuals do not have permanent immunity, and can progress back to the S_r, S_c and S_v classes at rate $\tau(1-(\eta_c+\eta_v))$, $\tau\eta_c$ and $\tau\eta_v$. The parameter δ represents natural death rate in each component and μ is the disease-related death rate. For the pathogen compartment, the concentration of cholera pathogen grows at rate g and decays at rate d. We let $\lambda = d - g$. From the schematic diagram in Figure 1, with

$$\varphi(t) = \rho_r I(t) + \beta_r B(t), \varphi_c(t) = \rho_c I(t) + \beta_c B(t), \varphi_v(t) = \rho_v I(t) + \beta_v B(t),$$

we obtain the following cholera model with cultural practices and vaccination:

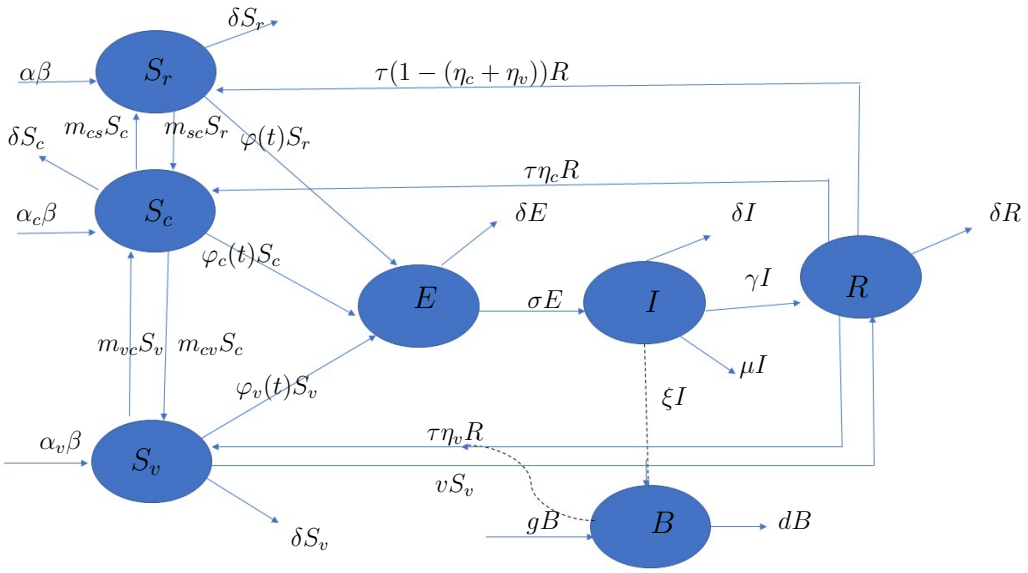

Figure 1. Flow diagram for the cholera model. Solid lines represent flow between compartments, the straight dashed line represents the infected class shedding pathogen into the environment, and the curved dashed line represents the source of new infections resulting from susceptible individuals interacting with the pathogen. All other arrows represent natural deaths, birth or growth of pathogen.

$$\begin{aligned}
\frac{dS_r}{dt} &= \alpha\beta - (\rho_r I + \beta_r B)S_r - (\delta + m_{sc})S_r + m_{cs}S_c + \tau(1-(\eta_c+\eta_v))R \\
\frac{dS_c}{dt} &= \alpha_c\beta - (\rho_c I + \beta_c B)S_c - (\delta + m_{cv} + m_{cs})S_c + m_{vc}S_v + m_{sc}S_r + \tau\eta_c R \\
\frac{dS_v}{dt} &= \alpha_v\beta - (\rho_v I + \beta_v B)S_v - (\delta + m_{vc})S_v + m_{cv}S_c + \tau\eta_v R - vS_v \\
\frac{dE}{dt} &= (\rho_r I + \beta_r B)S_r + (\rho_c I + \beta_c B)S_c + (\rho_v I + \beta_v B)S_v - (\sigma + \delta)E \\
\frac{dI}{dt} &= \sigma E - (\gamma + \mu + \delta)I \\
\frac{dR}{dt} &= \gamma I - (\delta + \tau)R + vS_v
\end{aligned} \tag{2.1}$$

$$\frac{dB}{dt} = \xi I - \lambda B,$$

with initial conditions:

$$S_r(0) > 0, S_c(0) > 0, S_v(0) > 0, E(0) \geq 0, I(0) \geq 0, R(0) \geq 0, B(0) \geq 0.$$

Table 1. Model variables, descriptions and units.

Variable	Description	Unit
S	Susceptible individuals	individuals
S_r	Susceptible individuals who are not careful and not willing to be vaccinated	individuals
S_c	Susceptible individuals who are careful but not willing to be vaccinated	individuals
S_v	Susceptible individuals who are careful and willing to be vaccinated	individuals
E	Exposed individuals	individuals
I	Infectious individuals	individuals
R	Recovered individuals	individuals
B	Pathogen concentration in water environment	cells ml^{-1}
N	Total population	individuals

From the B equation, when there is no shedding and $\lambda < 0$, we see that the pathogen maintains itself in the environment. In our application, $g - d = -0.33$ [18]. Consequently, we assume throughout that $\lambda = d - g > 0$.

To obtain the feasible region of solutions to model (2.1), we add the equations for S_r, S_c, S_v, E, I and R to obtain

$$\frac{dN}{dt} = \beta - \delta N - \mu I$$

and noting that $I(t) \geq 0$ for all t, we get

$$\frac{dN}{dt} \leq \beta - \delta N.$$

Thus

$$\limsup_{t\to\infty} N(t) \leq \frac{\beta}{\delta} = N_\infty.$$

Consequently, the B equation implies

$$\frac{dB}{dt} \leq \xi N_\infty - \lambda B,$$

and

$$\limsup_{t\to\infty} B(t) \leq \frac{\xi N_\infty}{\lambda} = B_\infty.$$

Assuming $0 \leq B(0) \leq B_\infty$, we have $B(t) \leq B_\infty$ for all $t \geq 0$. Then the feasible region of solutions of Model (2.1) is the compact set

$$\Omega = \{(S_r, S_c, S_v, E, I, R, B) \in \mathbf{R}^7_+ | 0 \leq S_r, S_c, S_v, E, I, R \leq N_\infty,\ 0 \leq B \leq B_\infty\ \}.$$

From the structure of our system of differential equations, with non-negative initial conditions the solutions can be shown to remain non-negative, and we have that the upper bounds in the feasible region are valid [19].

2.1. Model without culture and vaccination

When there are no cultural practices and no vaccination, and there is only one susceptible class S, Model (2.1) reduces to the following system of ordinary differential equations:

$$\begin{aligned}
\frac{dS}{dt} &= \beta - (\rho_s I + \beta_s B)S + \tau R - \delta S \\
\frac{dE}{dt} &= (\rho_s I + \beta_s B)S - (\sigma + \delta)E \\
\frac{dI}{dt} &= \sigma E - (\gamma + \mu + \delta)I \\
\frac{dR}{dt} &= \gamma I - (\delta + \tau)R \\
\frac{dB}{dt} &= \xi I - \lambda B.
\end{aligned} \tag{2.2}$$

with initial conditions:

$$S(0) = S_0 > 0, E(0) = E_0 \geq 0, I(0) = I_0 \geq 0, R(0) = R_0 \geq 0, B(0) = B_0 \geq 0.$$

In Model (2.1), ρ_s and β_s are the direct and indirect transmission rates, respectively. The disease-free equilibrium (DFE) for model (2.2) is

$$P_0 = (S^0, E^0, I^0, R^0, B^0) = (\beta/\delta, 0, 0, 0, 0)\,.$$

We use the next generation matrix (NGM) method to compute the basic reproduction number, $\mathcal{R}_0$ [13, 20–22]. Assuming that λi in the B differential equation is not a new infection, then by the NGM method,

$$\mathcal{R}_0 = \mathcal{R}_0^I + \mathcal{R}_0^B, \tag{2.3}$$

where

$$\mathcal{R}_0^I = \frac{\sigma\rho_s S^0}{(\sigma + \delta)(\gamma + \mu + \delta)} \quad \text{and} \quad \mathcal{R}_0^B = \frac{\xi\sigma\beta_s S^0}{\lambda(\sigma + \delta)(\gamma + \mu + \delta)}.$$

The basic reproduction number, $\mathcal{R}_0$, is the sum of two terms, $\mathcal{R}_0^I$ and $\mathcal{R}_0^B$, with $\mathcal{R}_0^I$ accounting for the infections from the infectious class, and $\mathcal{R}_0^B$ accounting for the infections from the contaminated environment. Consequently, if $\mathcal{R}_0 < 1$ then the DFE, P_0, is locally asymptotically stable, there is no cholera invasion, and the number of cholera infections eventually decrease. If $\mathcal{R}_0 > 1$, then P_0 is unstable, cholera invades the Far North Region of Cameroon and the number of cholera infections increases. We note that if $\mathcal{R}_0^I > 1$ or $\mathcal{R}_0^B > 1$, then $\mathcal{R}_0 > 1$. Furthermore, it is possible for $\mathcal{R}_0^I < 1$, $\mathcal{R}_0^B < 1$ but $\mathcal{R}_0 > 1$.

To compute $\mathcal{R}_0$ for the Far North Region of Cameroon, in Section 2.2, we use the daily reported cholera cases from the three health districts (Kaélé, Kar Hay and Moutourwa) in the Far North Region from June 25 to August 16, 2019, from the Cameroon Ministry of Public Health [17] to estimate the remaining Model (2.2) parameter values. We will use model (2.2) to illustrate that in the Far North Region of Cameroon, $\mathcal{R}_0 > 1$ and cholera is an endemic infectious disease.

2.2. Model without culture and vaccination: parameter estimation

Some model parameters are known from the literature and some are estimated from our data. The mean exposed period of cholera, $1/\sigma$, is between 12 hours to 5 days [1]. In our simulation $1/\sigma = 1.4$ days, the estimated value for the median exposed period of toxigenic cholera [23]. For the immune period, $1/\tau = 10^3$ days [24], for the net decay rate of pathogen, $\lambda = 0.33$ day^{-1}, and for the shedding rate $\xi = 10$ cells ml^{-1} day^{-1} individuals^{-1} [18]. For the mean infectious period, $1/\gamma = 5$ days [14, 25]. For the cholera-related death rate, $\mu = 5.5329 \times 10^{-4}$ per day [15]. We estimate the remaining model parameters using the multistart algorithm with the *fmincon* function in the MATLAB optimization toolbox. The fmincon function takes an iterative approach to solving an optimization problem that includes our parameter values as unknowns with the scalar value to be minimized being the relative error,

$$\text{Relative error} \quad = \quad \frac{\|YI(m) - YI^*\|_2}{\|YI^*\|_2}, \tag{2.4}$$

where $YI(m)$ is the vector of the cumulative number of daily infections given by the Model (2.2) with parameter vector $m = (\rho_s, \beta_s)$, and YI^* is the corresponding vector of the values of the cumulative daily reported cholera cases [17]. At time $t \geq 0$, the cumulative cases are computed by integrating the term σE in the I-equation of Model (2.2), from 0 to t, using the MATLAB solver ODE45. The total population of the three health districts in Far North Region as of August 17, 2019 is 89884 [17]. The time period of our simulation is 53 days (June 25, 2019 to August 16, 2019,), so $N(53) = 89884$. Here, $t \geq 0$ is in days and $t = 0$ corresponds to June 25, 2019 and $t = 53$ corresponds to August 16, 2019.

We let

$$\beta/\delta = N_\infty = N(53) = 89884,$$

so that $\beta = \delta \times 89884$. From Table 2, $\delta = \frac{9.1\times10^{-3}}{365}$ day^{-1}. Consequently, $\beta = \frac{817944.4\times10^{-3}}{365}$ day^{-1}. We choose $N(0)$ so that $N(0) < N(53)$. So we let $N(0) = 89548$. For the other initial conditions, we choose $E(0) = 0$, $I(0) = 1$, $R(0) = 0$, $S(0) = N(0) - (E(0) + I(0) + R(0))$. Similar initial conditions give similar results. As in [15], we take the total initial cholera bacteria concentration $B(0) = 1000$. Table 2 gives estimates for the remaining Model (2.2) parameter values, $\rho_s = 2.1737 \times 10^{-6}$ and $\beta_s = 1.8694 \times 10^{-8}$. Using these values and the known parameter values on Table 2, we obtain that $\mathcal{R}_0 = 1.2279 > 1$. That is, Model (2.1) predicts that cholera is endemic in the three health district Far North Region of Cameroon.

In Figure 2, we illustrate the daily cumulative number of new cholera infections predicted by Model (2.2) in comparison to the actual cumulative daily cholera reported cases in the three health districts (Kaélé, Kar Hay and Moutourwa) of the Far North Region of Cameroon from June 25 to August 16, 2019. From Figure 2, we see that with relative error 0.1623, Model (2.2) appears to predict an increasing trend in the cumulative number of daily cholera infections in the three health districts of the Far North Region of Cameroon, as in the actual reported cumulative cholera cases per day.

Table 2. Model without culture (Model (2.2)) parameters, descriptions and values.

Parameter	Description	Value	Source
β	constant recruitment rate	$\frac{817944.4\times10^{-3}}{365}$ day^{-1}	estimated
δ	natural death rate	$\frac{9.1\times10^{-3}}{365}$ day^{-1}	[26]
ρ_s	direct transmission rate between S and I	2.1737×10^{-6}day^{-1}	estimated
β_s	indirect transmission rate between S and I	1.8694×10^{-8} day^{-1}	estimated
$1/\tau$	immune period	10^3 days	[24]
$1/\sigma$	mean exposed period	1.4 days	[23]
$1/\gamma$	mean infectious period	5 days	[14, 25]
μ	cholera-related death rate	5.5329×10^{-4} days	[15]
ξ	shedding rate of pathogens by I	10 cells ml^{-1}day^{-1}individual^{-1}	[18]
λ	net decay rate of pathogen	0.33 day^{-1}	[18]

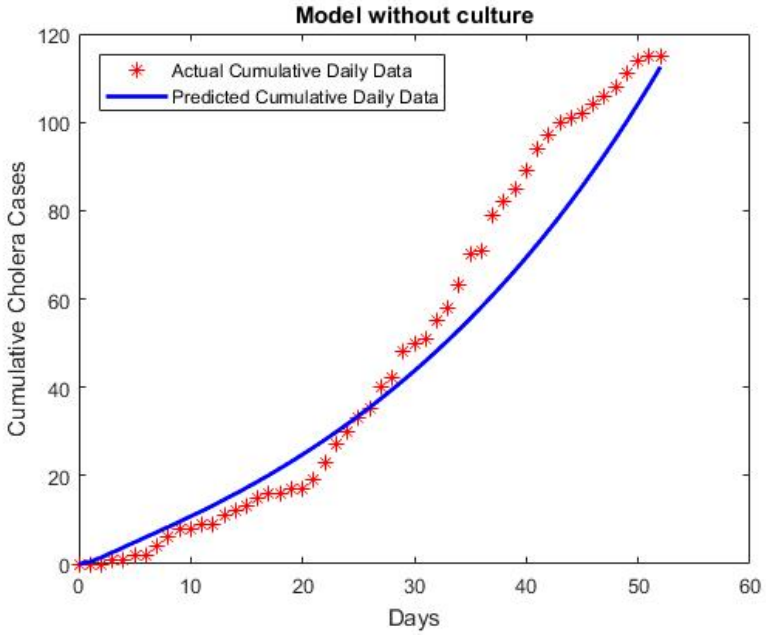

Figure 2. Scatterplot of the cumulative values of cholera disease cases in the three health districts (Kaélé, Kar Hay and Moutourwa) of the Far North Region of Cameroon per day for June 25 to August 16, 2019 from [17] plotted against simulation output using estimated parameters.

2.3. Model with culture: DFE and $\mathcal{R}_c$

In order to compute the disease-free equilibrium (DFE) of the structured model with cultural practices, we introduce the following notation:

$$\begin{aligned} A &= \delta + m_{sc}, \quad C = \tau(1 - (\eta_c + \eta_v)), \quad D = \delta + m_{cv} + m_{cs}, \\ F &= \delta + m_{vc} + v, \quad J = \delta + \tau, \quad K = \alpha\beta, \\ L &= \alpha_c\beta, \quad M = \alpha_v\beta, \quad P = JF - \tau\eta_v v, \end{aligned}$$

$$\begin{aligned} S_N &= Jm_{sc}m_{cs}M - Jm_{cv}m_{sc}K - AJDM - AJm_{cv}L \\ S_D &= AJm_{cv}m_{vc} + m_{sc}(m_{cs}P + m_{cv}Cv) + Am_{cv}\tau\eta_c v - ADP \end{aligned}$$

Thus, the DFE of model (2.1) is

$$P_c = (S_r^c, S_c^c, S_v^c, E^c, I^c, R^c, B^c) = (S_r^c, S_c^c, S_v^c, 0, 0, R^c, 0),$$

where

$$\begin{aligned} S_v^c &= \frac{S_N}{S_D}, \\ S_r^c &= \frac{K}{A} - \frac{m_{cs}M}{Am_{cv}} + \left(\frac{m_{cs}P + m_{cv}Cv}{AJm_{cv}}\right) S_v^c, \\ S_c^c &= \left(\frac{P}{Jm_{cv}}\right) S_v^c - \frac{M}{m_{cv}}, \\ R^c &= \frac{v}{J} S_v^c \end{aligned}$$

As in the model without culture, using the next generation matrix (NGM) method, we compute $\mathcal{R}_c$, the control reproduction number. Assuming that λi is not a new infection,

$$\mathcal{R}_c = \mathcal{R}_c^I + \mathcal{R}_c^B, \tag{2.5}$$

where

$$\mathcal{R}_c^I = \frac{\sigma(\rho_r S_r^c + \rho_c S_c^c + \rho_v S_v^c)}{(\sigma+\delta)(\gamma+\mu+\delta)} \quad \text{and} \quad \mathcal{R}_c^B = \frac{\sigma\xi(\beta_r S_r^c + \beta_c S_c^c + \beta_v S_v^c)}{\lambda(\sigma+\delta)(\gamma+\mu+\delta)}.$$

Again, as in the Model without cultural practices, the control reproduction number, $\mathcal{R}_c$, is the sum of two terms, $\mathcal{R}_c^I$ and $\mathcal{R}_c^B$. $\mathcal{R}_c^I$ accounts for the infections from the infectious class, and $\mathcal{R}_c^B$ accounts for the infections from the contaminated environment.

In Section 2.4, we compute $\mathcal{R}_c$ for the Far North Region of Cameroon using the daily reported cholera cases from the three health districts (Kaélé, Kar Hay and Moutourwa) in the Far North Region from June 25, 2019 to August 16, 2019 [17], and estimate the remaining parameter values of model (2.1). Again, we will use model (2.1) to illustrate that in the Far North Region of Cameroon, $\mathcal{R}_c < 1$ and with vaccination, cholera can be eradicated. Moreover, we will use AIC to illustrate that model (2.1) better captures the impact of cultural practices on the dynamics of cholera infections in the three health districts (Kaélé, Kar Hay and Moutourwa) in the Far North Region, which is in agreement with the results of the field work in [8].

2.4. Parameter Estimation

As in model (2.2), we estimate the remaining model parameters using the multistart algorithm with the *fmincon* built-in function in the MATLAB optimization toolbox. In equation (2.4), $YI(m)$ is the vector of the cumulative number of daily infections given by model (2.1) with parameter vector m, and YI^* is the corresponding vector of the values of the cumulative daily reported cholera cases [17].

Again, as in Model (2.2),at time $t \geq 0$, the cumulative cases are computed by integrating the term σE in the I-equation of Model (2.1), from 0 to t, using the MATLAB solver ODE45. Also, as in Model (2.2) $N(0) = 89548$. For the other initial conditions, we choose the initial susceptible population so that $S_r(0) > S_c(0) > S_v(0)$. Consequently, we start with $S_c(0) = 4500$, $S_v(0) = 2100$ $E(0) = 0$, $I(0) = 1$, $R(0) = 0$, $S_r(0) = N(0) - (S_c(0) + S_v(0) + I(0) + E(0) + R(0))$. Similar initial conditions give similar results. As in [15], we take the total initial cholera bacteria concentration $B(0) = 1000$.

In our simulations, to capture the fact that susceptible individuals in the S_r class (who because of their cultural beliefs are not careful in practicing safe cholera intervention measures and not willing to be vaccinated) have higher direct transmission rates than those in the S_c and S_v classes, we let $\rho_c < \rho_r$ and $\rho_v < \rho_r$.

Table 3 gives estimates for the remaining parameter values of model (2.1). Using these parameter values and equation (2.5), we estimate that $\mathcal{R}_c = 0.0873 < 1$. That is, model (2.1) predicts that with vaccination, cholera can be eradicated in the three health district Far North Region of Cameroon. In Figure 3, we illustrate the daily cumulative number of new cholera infections predicted by Model (2.1) in comparison to the actual cumulative daily cholera reported cases in the three health districts (Kaélé, Kar Hay and Moutourwa) of the Far North Region of Cameroon for June 25 to August 16, 2019.

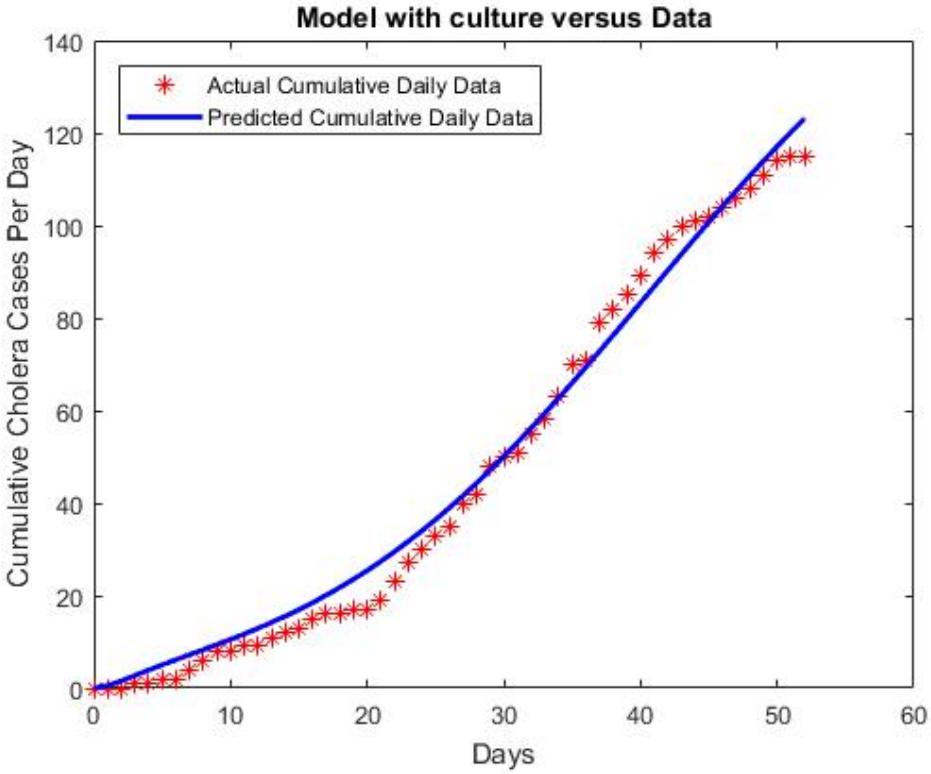

Figure 3. Scatterplot of the cumulative values of cholera disease cases in the three health districts (Kaélé, Kar Hay and Moutourwa) of the Far North Region of Cameroon per day for June 25 to August 16, 2019 from [17] plotted against simulation output using estimated parameters. With the relative error 0.0676 and $\mathcal{R}_c = 0.0873 < 1$, model (2.1) is predicting an increasing trend in the daily number of cumulative cholera infections, like in the observed cumulative number of cholera infections.

Table 3. Model with culture (Model (2.1)) parameters, descriptions and values.

Parameter	Description	Value	Source
β	constant recruitment rate	$\frac{817944.4\times10^{-3}}{365}$ day^{-1} day^{-1}	estimated
δ	natural death rate	$\frac{9.1\times10^{-3}}{365}$ day^{-1}	[26]
ρ_r	direct transmission rate between S_r and I	3.0043×10^{-8}day^{-1}	estimated
ρ_c	direct transmission rate between S_c and I	2.9990×10^{-8} day^{-1}	estimated
ρ_v	direct transmission rate between S_v and I	1.3225×10^{-9} day^{-1}	estimated
β_r	indirect transmission rate between S_r and I	1.0023×10^{-11} day^{-1}	estimated
β_c	indirect transmission rate between S_c and I	1.0002×10^{-10} day^{-1}	estimated
β_v	indirect transmission rate between S_v and I	1.0×10^{-6} day^{-1}	estimated
$1/\tau$	immune period	10^3 days	[24]
$1/\sigma$	mean exposed period	1.4 days	[23]
$1/\gamma$	mean infectious period	5 days	[14, 25]
μ	cholera-related death rate	5.5329×10^{-4} days	[15]
ξ	shedding rate of pathogens by I	10 cells ml^{-1}day^{-1}individual^{-1}	[18]
λ	net decay rate of pathogen	0.33 day^{-1}	[18]
m_{sc}	transition rate from S_r to S_c	0.1538day^{-1}	estimated
m_{cs}	transition rate from S_c to S_r	0.0001day^{-1}	estimated
m_{cv}	transition rate from S_c to S_v	0.03 day^{-1}	estimated
m_{vc}	transition rate from S_v to S_c	0.0001 day^{-1}	estimated
η_c	fraction of waning immunity from R to S_c	0.0523	estimated
η_v	fraction of waning immunity from R to S_v	0.70004	estimated
α	fraction of recruitment rate into S_r	0.9546	estimated
α_c	fraction of recruitment rate into S_c	0.0321	estimated
α_v	fraction of recruitment rate into S_v	0.0133	estimated
v	vaccination rate of S_v	0.1568	estimated

To compare our model without culture to the model with culture, in addition to their relative errors, we compute correct Akaike information criterion (AIC),

$$\text{AIC} \quad = \quad n\log\left(\frac{\sum_{i=1}^{n}(YI^*(i)-YI(i))^2}{n}\right)+2k,$$

where n is the number of days of the cholera infection, and for $i = 1,\ldots,n$, $YI^*(i)$ is of the actual cumulative number of daily reported cholera cases [17] and $YI(i)$ is the cumulative number of daily infections given by our model, and k is the number of estimated parameters [27]. Table 4 summarizes the relative and AIC values for the model without culture and the model with culture.

From Table 4, we see that in comparison to the Model without culture, our Model with culture gives us a smaller relative error and AIC value.

From Figures 2 and 3, we see that as in the actual reported cumulative cholera cases, both models without culture and with culture appear to predict an increasing trend in the cumulative number of daily cholera infections in the three health districts of the Far North Region of Cameroon. However, the model with culture (model (2.1)) gives us a better fit than the model without culture (model (2.2)),

Table 4. Comparative model fit for the two models.

	Model without culture	Model with culture
n	53	53
k	2	16
Relative error	0.1623	0.0676
AIC	109.9247	97.6018

with a smaller relative error 0.0676 and smaller AIC=97.6018. Thus, our model (2.1) captures the influence of cultural practices on the spread of cholera infections in the Far North Region as reported in [8].

3. Sensitivity analysis and the effects of cultural practices on the spread of cAholera

In this section, we use sensitivity analysis to study the impact of each model parameter on the threshold parameter, $\mathcal{R}_c$, and the number of model predicted cholera cases. We also explore the effect of cultural practices on the spread of cholera by generating contour plots of the basic reproduction number ($\mathcal{R}_c$) with respect to two of the parameters in Table 3.

3.1. Relative Sensitivity Indices of $\mathcal{R}_c$

For a variable v and a parameter p, the *relative sensitivity index* to the parameter p is defined as

$$\Upsilon_p^v = \frac{\partial v}{\partial p} \times \frac{p}{v}.$$

This index gives the proportional rate of change of v as p changes [28]. We compute the relative sensitivity indices for $\mathcal{R}_c$ with respect to each of the parameters of Table 3. Most of the relative sensitivity indices are complicated algebraic expressions with no obvious structure. As in [28], we evaluate the relative sensitivity indices at the baseline parameter values given in Table 3. Table 5 summarizes our results, with the parameters ordered from the most sensitive β to the least sensitive β_r. From Table 5, $\Upsilon_\beta^{\mathcal{R}_c} = +1.000$. Thus, decreasing (or increasing) the most sensitive parameter β, the constant recruitment rate, by 10% decreases (or increases) $\mathcal{R}_c$ by 10.0000%. The least sensitive parameter is β_r, the indirect transmission rate between the S_r and I classes. Because

$$\Upsilon_{\beta_r}^{\mathcal{R}_c} = +2.7131 \times 10^{-6},$$

decreasing (or increasing) β_r by 10% decreases (or increases) $\mathcal{R}_c$ by $+2.7131 \times 10^{-5}$%.

3.2. Global sensitivity analysis

We perform a global sensitivity analysis for our model using Latin Hypercube Sampling (LHS) to sample the parameter space and Partial Rank Correlation Coefficients (PRCC) to evaluate the sensitivity of the outcome variable, the total number of model predicted cholera cases, to uncertainty in the input variables [29–31]. For parameter intervals, we chose to go 50% above and below the values in Table 3. Uniform probability distributions were used for each parameter interval. From the recommendation in [32], we take $N > 4M/3$ draws of the LHS design, where M is the number of input

parameters and N is the number of LHS draws. In our case, $M = 24$ and $N = 80$. Table 6 gives the PRCCs and the p-values for each model parameter while Figure 4 show p-values of the sensitivity of the number of cholera cases to changes in parameters in Table 6 as computed by the Latin Hypercube Sampling-Partial Rank Correlation Coefficient (LHS-PRCC) index. Based on the p-values, we observe that PRCC values for β_v, 0.5956; σ, 0.8981; ξ, 0.5172; λ, −0.9749 and v, 0.5769 are statistically significant. The parameters β_v, σ, ξ and v show a significant positive correlation with the total number of cholera cases while λ shows a significant negative correlation with the total number of cholera cases. This is in agreement with our model predictions.

Table 5. Sensitivity indices of $\mathcal{R}_c$ with respect to the parameters of Model (2.1), evaluated at the baseline parameter values given in Table 3.

Parameter	Sensitivity Index
β	+1.0000
ξ	$+9.9805 \times 10^{-1}$
λ	-9.9805×10^{-1}
β_v	$+9.9788 \times 10^{-1}$
γ	-9.9712×10^{-1}
v	-9.9149×10^{-1}
δ	-9.7684×10^{-1}
τ	$+9.5790 \times 10^{-1}$
α	$+9.5459 \times 10^{-1}$
α_c	$+3.2084 \times 10^{-2}$
η_v	$+2.2814 \times 10^{-2}$
α_v	$+1.3321 \times 10^{-2}$
m_{cv}	$+8.8344 \times 10^{-3}$
μ	-2.7585×10^{-3}
ρ_c	$+1.6370 \times 10^{-3}$
m_{sc}	$+1.4683 \times 10^{-3}$
η_c	$+2.8175 \times 10^{-4}$
ρ_r	$+2.6835 \times 10^{-4}$
β_c	$+1.6544 \times 10^{-4}$
ρ_v	$+4.3551 \times 10^{-5}$
σ	$+3.4903 \times 10^{-5}$
m_{vc}	-1.8273×10^{-5}
m_{cs}	-5.9587×10^{-6}
β_r	$+2.7131 \times 10^{-6}$

Table 6. Model parameters, corresponding PRCC and corresponding p-values resulting from the sensitivity analysis. Significant p-values ($p < 0.01$) are bold-faced.

Parameter	PRCC	P-value
β	−0.1709	0.2037
δ	0.07418	0.5837
ρ_r	−0.0469	0.7289
ρ_c	−0.0689	0.6101
ρ_v	0.0371	0.7839
β_r	−0.0117	0.9311
β_c	−0.0184	0.8920
β_v	0.5956	**0.0000**
τ	−0.0594	0.6607
σ	0.8981	**0.0000**
γ	−0.1973	0.1413
μ	0.1574	0.2422
ξ	0.5172	**0.0000**
λ	−0.9749	**0.0000**
m_{sc}	0.1983	0.1392
m_{cs}	0.0366	0.7867
m_{cv}	0.1186	0.3794
m_{vc}	0.1864	0.1649
η_c	−0.2564	0.8499
η_v	−0.0269	0.8426
α	−0.1351	0.3163
α_c	−0.0159	0.9061
α_v	−0.0095	0.9438
v	0.5769	**0.0000**

3.3. Effects of Cultural Beliefs on cholera

In this section, we explore the effects of cultural practices on the spread of cholera by generating a contour plot of the control reproduction number ($\mathcal{R}_c$) with respect to the two parameters, m_{cs} and m_{cv}, in Table 3.

A contour plot of the reproduction number, $\mathcal{R}_c$, as a function of the transition rates m_{cs} (from S_c to S_r) and m_{cv} (from S_c to S_v) is depicted in Figure 5. Using the parameter values in Table 3, our contour plot indicates that an increase in the transition rate of susceptible individuals from being careful in practicing safe cholera intervention measures but unwilling to be vaccinated (S_c) to those who are not careful in practicing safe cholera intervention measures and not willing to be vaccinated (S_r), and a decrease in the transition rate of susceptible individuals from being careful in practicing safe cholera intervention measures but unwilling to be vaccinated (S_c) to those who are careful in practicing safe cholera intervention measures and are willing to be vaccinated (S_v) results in a control reproduction number of $\mathcal{R}_c = 0.09 < 1$. Even though there seem to be an increase in the control reproduction

number, $\mathcal{R}_c$ is smaller than 0.1, which corroborates with our data.

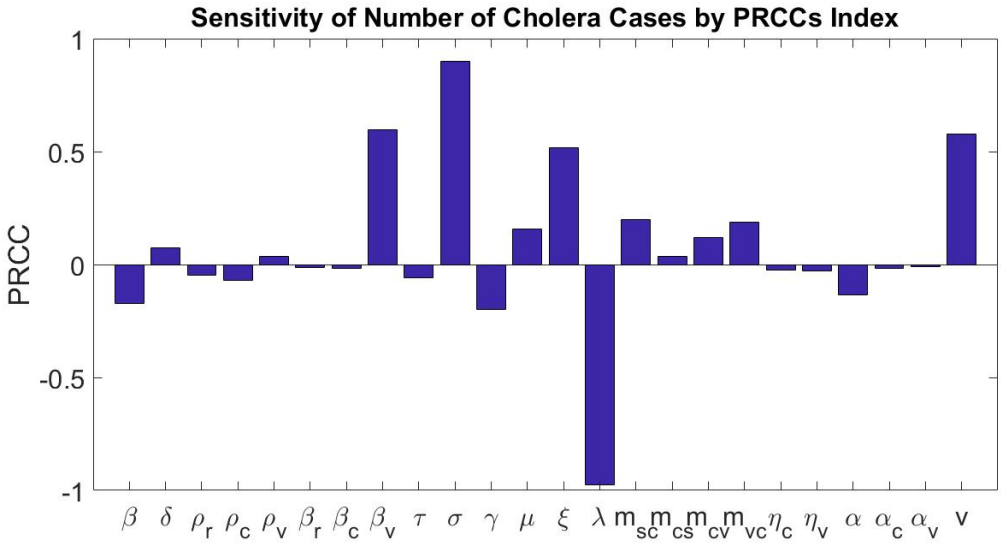

Figure 4. Sensitivity of the number of cholera cases to changes in parameters in Table 3 as computed by the Latin Hypercube Sampling-Partial Rank Correlation Coefficient (LHS-PRCC) index.

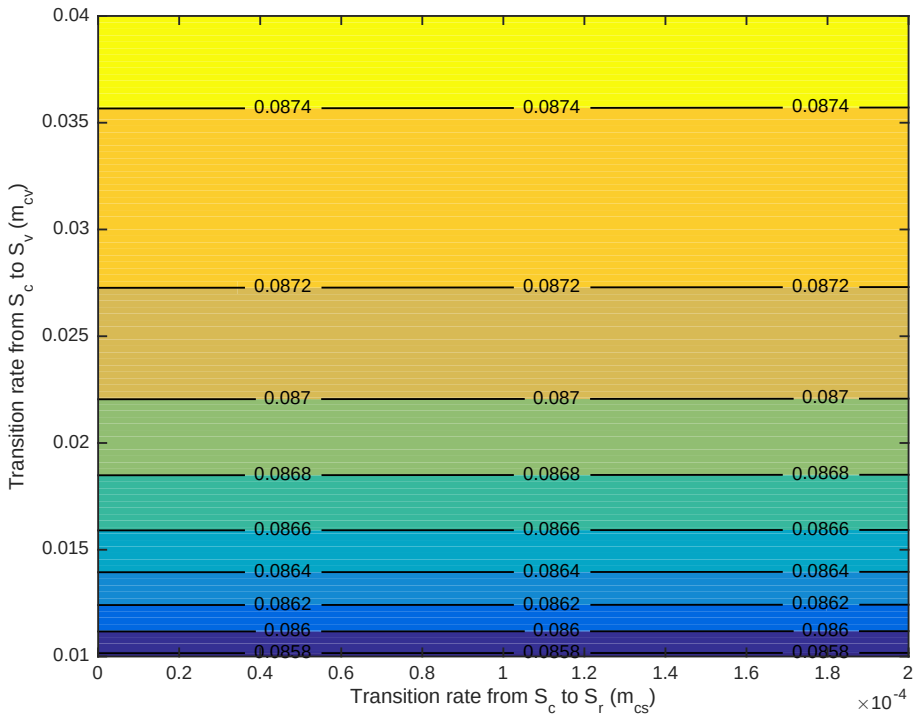

Figure 5. Contour plot of $\mathcal{R}_c$ as a red function of m_{cs} and m_{cv}.

4. Conclusions

We introduced a model for the dynamics of cholera in the Far North Region of Cameroon that captures cultural practices and vaccination of cholera in the Far North Region. Our model incorporates direct (human-to-human) and indirect (contaminated water-to-human) infection pathways. We use our model to capture the reported cholera cases in the three health districts (Kaélé, Kar Hay and Moutourwa) of the Far North Region of Cameroon from June 25 to August 16, 2019. Using our model parameters we obtain that the control reproduction number $\mathcal{R}_c < 1$, and our model with cultural practices and vaccination predicts that cholera can be eradicated. The AIC shows that our model with cultural practices and vaccination appears to be a better fit to cumulative number of daily cholera infections in the three health districts of the Far North Region of Cameroon. Consequently, we use model (2.1) to study the effect of cultural practices on cholera cases [8].

We perform sensitivity analysis to determine the impact of each model parameter on the threshold parameter, $\mathcal{R}_c$, and on the total number of model predicted cholera cases in in the three health districts (Kaélé, Kar Hay and Moutourwa) of the Far North Region of Cameroon for June 25 to August 16, 2019. For $\mathcal{R}_c$, the most sensitive parameter is β (constant recruitment rate), and the least sensitive parameter β_r, the indirect transmission rate between the S_r and I classes. The statistically significant parameters to the number of model predicted cholera cases are β_v, σ, ξ, λ and v. The parameters β_v, σ, ξ and v show a significant positive correlation with the total number of cholera cases while λ shows a significant negative correlation with the total number of cholera cases. This is in agreement with our model predictions.

A contour plot for the control reproduction number as a function of transition rates between different compartments of susceptible individuals suggests that as humans transition from a class of susceptible individuals who are careful in practicing safe cholera intervention measures but unwilling to be vaccinated (S_c) to those who are not careful in practicing safe cholera intervention measures and not willing to be vaccinated (S_r), the control reproduction number is below one. Thus, our work suggests that in the Far North Region of Cameroon, while implementing intervention schemes such as education and vaccination, public health officials should take into account cultural practices in the region. Since some of the cultural practices stem from religious beliefs of the populace, public health officials should consider working with local chiefs and religious priests when designing the intervention schemes for the control of cholera in the region.

Our models do not take into account the impact of the cost of intervention strategies on the number of cholera infections. In addition to demonstrating that cultural practices in the Far North region influence cholera transmission, Ngwa *et al.* in [8] also noted that many people in the Far North had limited scientific knowledge about the cholera disease and its transmission. As more data becomes available, a study of a cholera model that captures education and cultural practices, and cost analysis of intervention strategies in the Far North Region of Cameroon will be an interesting extension of this work.

Conflict of interest

The authors declare there is no conflict of interests.

References

1. WHO, Cholera, available from: https://www.who.int/immunization/diseases/cholera/en/.
2. WHO, Weekly Epidemiological Record, No 36, (2017), 92, 521–536, available from: http://www.who.int/wer.
3. D. Posny, C. Modnak, J. Wang, A multigroup model for cholera dynamics and control, *Int. J. Biomath.*, **9** (2016), 1650001.
4. M. Ali, A. R. Nelson, A. L. Lopez, D. A. Sack, Updated Global Burden of Cholera in Endemic Countries, *PLoS Negl. Trop. Dis.*, **9** (2015), e0003832.
5. UNICEF, Cholera epidemiology and response factsheet Cameroon, available from https://www.unicef.org/cholera/files/UNICEF-Factsheet-Cameroon-EN-FINAL.pdf.
6. WHO, Cholera, available from: https://www.who.int/news-room/fact-sheets/detail/cholera.
7. A. Manguvo, B. Mafuvadze, The impact of traditional and religious practices on the spread of Ebola in West Africa: time for a strategic shift, *Pan Afr. Med. J.*, **22** (2015), 9.
8. M. C. Ngwa, A. Young, S. Liang, J. Blackburn, A. Mouhaman, J. G. Morris, Cultural influences behind cholera transmission in the Far North Region, Republic of Cameroon: a field experience and implications for operational level planning of interventions, *Pan Afr. Med. J.*, **08** (2017), 311.
9. M. K. Nfor, Recurrent Cholera Outbreak in Far North Cameroon Highlights Development Gaps, *Reliefweb*, 2014, available from: https://reliefweb.int/report/cameroon/recurrent-cholera-outbreak-far-north-cameroon-highlights-development-gaps
10. K. R. Fister, H. Gaff, S. Lenhart, E. Numfor, E. Schaefer, J. Wang, Optimal Control of Vaccination in an Age-structured Cholera Model, In: Chowell G., Hyman J. (eds), *Mathematical Modeling of Emerging and Re-emerging Infectious Diseases*, Springer, Cham, (2016), 221–248.
11. M. R. Kelly, J. H. Tien, M. C. Eisenberg, S. Lenhart, The impact of spatial arrangements on the epidemic disease dynamics and intervention strategies, *J. Biol. Dyn.*, **10** (2016), 222–249.
12. J. H. Tien, D. J. D. Earn, Multiple transmission pathways and disease dynamics in a waterborne pathogen model, *Bull. Math. Biol.*, **72** (2010), 1502–1533.
13. P. van den Driessche. Reproduction numbers of infectious disease models, *Infect. Dis. Model.*, **2** (2017), 288–303.
14. J. Wang, C. Modnak, Modeling Cholera Dynamics with Controls, *Canadian Appl. Math. Q.*, **19** (2011), 255–273.
15. E. Che, Y. Kang, A. Yakubu, Risk structured model of cholera infections in Cameroon, *Math. Biosci.*, **320** (2020), 108303.
16. M. Al-arydah, A. Mwasa, J. M. Tchuenche, R. J. Smith, Modeling Cholera Disease with Education and Chlorination, *J. Biol. Syst.*, **21** (2013), 1340007.
17. Ministry of Public Health Cameroon, Rapport de situation N^{o}10 Épidémie de choléra dans la région de l'Extrême-Nord, 17 août 2019. Available from https://reliefweb.int/report/cameroon/rapport-de-situation-n-10-pid-mie-de-chol-ra-dans-la-r-gion-de-l-extr-me-nord-17-ao.

18. C. T. Codeço, Endemic and epidemic dynamics of cholera: the role of the aquatic reservoir, *BMC Infect. Dis.*, **1** (2001), no. 1.
19. N. Siewe, A. A. Yakubu, A. R. Satoskar, A. Friedman. Immune response to infection by leishmania: A mathematical model, *Math. Biosci.*, **276** (2016), 28–43.
20. O. Diekmann, J. P. Heesterbeek, *Mathematical epidemiology of infectious diseases*, Wiley, (2000).
21. O. Diekmann, H. Heesterbeek, T. Britton, *Mathematical tools for understanding infectious disease dynamics*, Princeton University Press, (2012).
22. P. van den Driessche, J. Watmough, Reproduction numbers and sub-threshold endemic equilibria for compartmental models of disease transmission, *Math. Biosci.*, **180** (2002), 29–48.
23. A. S. Azman, K. E. Rudolph, D. A. T. Cummings, J. Lessler, The incubation period of cholera: A systematic review, *J. Infect.*, **66** (2013), 432–438.
24. M. Bani-Yaghoub, R. Gautam, Z. Shuai, P. van den Driessche, R. Ivanek, Reproduction numbers for infections with free-living pathogens growing in the environment, *J. Biol. Dyn.*, **6** (2012), 923–940.
25. D. M. Hartley, J. G. Morris Jr., D. L. Smith, Hyperinfectivity: A critical element in the ability of V. cholerae to cause epidemics?, *PLoS Med.*, **3** (2005), e7.
26. Knoema, World Data Atlas, Cameroon. Available from: https://knoema.com/atlas/Cameroon.
27. K. L. Webster, I. F. Creed, M. D. Skowronski, Y. H. Kaheil, Comparison of the Performance of Statistical Models that Predict Soil Respiration from Forests, *Soil Sci. Soc. Am. J.*, **73** (2009), 1157–1167.
28. N. Chitnis, J. M. Hyman, J. M. Cushing, Determining Important Parameters in the Spread of Malaria Through the Sensitivity Analysis of a Mathematical Model, *Bull. Math. Biol.*, **70** (2008), 1272–1296.
29. S. M. Blower, H. Dowlatabadi, Sensitivity and uncertainty analysis of complex models of disease transmission: an HIV model, as an example, *Int. Stat. Rev.*, **62** (1994), 229–243.
30. C. Edholm, B. Levy, A. Abebe, T. Marijani, S. Le Fevre, S. Lenhart, et al., A Risk-Structured Mathematical Model of Buruli Ulcer Disease in Ghana. In Kaper H., Roberts F. (eds) *Math. Planet Earth*, Springer, Cham, **5** (2019), 109–128.
31. S. Marino, I. B. Hogue, C. J. Ray, D. E. Kirschner, A methodology for performing global uncertainty and sensitivity analysis in systems biology, *J. Theor. Biol.*, **254** (2008), 178–196.
32. M. D. McKay, R. J. Beckman, W. J. Conover, A comparison of three methods for selecting values of input variables in the analysis of output from a computer code, *Technometrics*, **21** (1979), 239–245.
33. L. Allen, P. van den Driessche, The basic reproduction number in discrete-time epidemic models, *J. Differ. Equ. Appl.*, **14** (2008), 1127–1147.

AIMS Press